Mechanics and Materials Center
TEXAS A&M UNIVERSITY
College Station, Texas

PREDICTED AXIAL TEMPERATURE GRADIENT IN A VISCOPLASTIC UNIAXIAL BAR DUE TO THERMOMECHANICAL COUPLING

BY

D. H. ALLEN

MM 4875-84-15

NOVEMBER 1984

ASIAC 14370

SECURITY CLASSIFICATION OF THIS PAGE

REPORT DOCUMENTATION PAGE

1a. REPORT SECURITY CLASSIFICATION unclassified	1b. RESTRICTIVE MARKINGS NA
2a. SECURITY CLASSIFICATION AUTHORITY NA	3. DISTRIBUTION/AVAILABILITY OF REPORT Unlimited
2b. DECLASSIFICATION/DOWNGRADING SCHEDULE NA	
4. PERFORMING ORGANIZATION REPORT NUMBER(S) MM 4875-84-15	5. MONITORING ORGANIZATION REPORT NUMBER(S) NA
6a. NAME OF PERFORMING ORGANIZATION Aerospace Engineering Dept.	6b. OFFICE SYMBOL (If applicable) NA
6c. ADDRESS (City, State and ZIP Code) College Station, TX 77843	7a. NAME OF MONITORING ORGANIZATION Air Force Office of Scientific Research
	7b. ADDRESS (City, State and ZIP Code) Washington, D.C. 20332
8a. NAME OF FUNDING/SPONSORING ORGANIZATION Air Force Office of Scientific Research	8b. OFFICE SYMBOL (If applicable)
8c. ADDRESS (City, State and ZIP Code) Washington, D.C. 20332	9. PROCUREMENT INSTRUMENT IDENTIFICATION NUMBER NA
	10. SOURCE OF FUNDING NOS.

PROGRAM ELEMENT NO.	PROJECT NO.	TASK NO.	WORK UNIT NO.

11. TITLE (Include Security Classification) Predicted Axial Temp. Gradient in a Viscoplastic Uniaxial Bar Due

12. PERSONAL AUTHOR(S)
David H. Allen

13a. TYPE OF REPORT	13b. TIME COVERED	14. DATE OF REPORT (Yr., Mo., Day)	15. PAGE COUNT
Interim	FROM _____ TO _____	November 1984	

16. SUPPLEMENTARY NOTATION

17. COSATI CODES		
FIELD	GROUP	SUB. GR.

18. SUBJECT TERMS (Continue on reverse if necessary and identify by block number)

19. ABSTRACT (Continue on reverse if necessary and identify by block number)

The thermomechanical response of a uniaxial bar with thermoviscoplastic constitution is predicted herein using the finite element method. After a brief review of the governing field equations, variational principles are constructed for the one dimensional conservation of momentum and energy equations. These equations are coupled in that the temperature field affects the displacements and vice versa.

Due to the differing physical nature of the temperature and displacements, first order and second order elements are utilized for these variables, respectively. The resulting semi-discretized equations are then discretized in time using finite differencing. This is accomplished by Euler's method, which is utilized due to the stiff nature of the constitutive equations.

The model is utilized in conjunction with with stress-strain relations developed by Bodner and Partom to predict the axial temperature field in a bar subjected to cyclic mechanical end displacements and temperature boundary conditions. It is found that

20. DISTRIBUTION/AVAILABILITY OF ABSTRACT	21. ABSTRACT SECURITY CLASSIFICATION
UNCLASSIFIED/UNLIMITED ☒ SAME AS RPT. ☐ DTIC USERS ☐	Unclassified

22a. NAME OF RESPONSIBLE INDIVIDUAL	22b. TELEPHONE NUMBER (Include Area Code)	22c. OFFICE SYMBOL
David H. Allen		

DD FORM 1473, 83 APR EDITION OF 1 JAN 73 IS OBSOLETE.

SECURITY CLASSIFICATION OF THIS PAGE

PREDICTED AXIAL TEMPERATURE GRADIENT IN A VISCOPLASTIC UNIAXIAL BAR DUE TO THERMOMECHANICAL COUPLING

by

D.H. Allen
Assistant Professor
Aerospace Engineering Department
Texas A&M University
College Station, TX 77843

MM 4875-84-15

November 1984

ABSTRACT

The thermomechanical response of a uniaxial bar with thermoviscoplastic constitution is predicted herein using the finite element method. After a brief review of the governing field equations, variational principles are constructed for the one dimensional conservation of momentum and energy equations. These equations are coupled in that the temperature field affects the displacements and vice versa.

Due to the differing physical nature of the temperature and displacements, first order and second order elements are utilized for these variables, respectively. The resulting semi-discretized equations are then discretized in time using finite differencing. This is accomplished by Euler's method, which is utilized due to the stiff nature of the constitutive equations.

The model is utilized in conjunction with stress-strain relations developed by Bodner and Partom to predict the axial temperature field in a bar subjected to cyclic mechanical end displacements and temperature boundary conditions. It is found that spacial and time variation of the temperature field is significantly affected by the boundary conditions.

TABLE OF SYMBOLS

t - time

P - axial internal resultant force

p_x - axial externally applied force per unit length

x - axial coordinate dimension

σ - axial stress component

A - cross-sectional area

T_x - end traction in units of force per unit area

s - surface area

Table of Symbols (cont.)

S_c - area of the longitudinal surface of the bar

ε - axial strain component

u - axial displacement component

α_1 - internal state variable representing axial inelastic strain

E - Young's modulus in the axial coordinate direction

α - coefficient of thermal expansion in the axial coordinate direction

T - temperature

T_R - reference temperature at which no deformation is observed at zero load

α_2 - internal state variable representing drag stress

q - axial component of heat flux

k - coefficient of axial thermal conductivity

C_v - specific heat at constant elastic strain

ρ - mass density

r - internal heat source per unit mass

L - length of the bar

INTRODUCTION

It is well known that mechanical and thermodynamic coupling are significant in metallic solids [1-11]. The author has recently developed a model capable of predicting this coupling effect in thermoviscoplastic metals [12]. In the previous paper a cyclic strain control loading on a sample of IN100 at 1005°K (1350°F) was used to predict a temperature rise of approximately 3.7°K per cycle when the strain amplitude was 2% and the specimen was adiabatically insulated.

The focus of the current research is to consider the effect of thermal boundary conditions on this same process. The introduction of these

conditions causes the strain and temperature fields to be inhomogeneous even though the stress field is homogeneous if the bar is prismatic. This spacial variation in the field variables causes the process to be difficult to model because the thermomechanical constitutive equations are highly nonlinear stiff differential equations. In this paper the finite element method is utilized to spatially discretize the dependent variables displacement and temperature, and the finite difference method is employed for timewise discretization. This process results in a set of highly nonlinear algebraic equations.

Since the thrust of this research is to obtain accurate results without regard to numerical efficiency, the results are obtained via the relatively inefficient but accurate method of simply utilizing successively smaller time steps along with refined spatial mesh to obtain a convergent and therefore accurate solution for the temperature and displacement fields both spatially and as a function of time for a cyclically imposed end displacement.

The physical interest in the problem is to determine the effect of temperature boundary conditions on the predicted temperature rise in a bar subjected to cyclic mechanical loading. It is found from the analysis that the introduction of these nonadiabatic boundary conditions causes significant axial temperature gradients. Since nonadiabatic conditions cannot be avoided in experimental research, it is concluded that experimental tests of this type should be viewed with caution when their purpose is to construct constitutive relations.

PROBLEM SOLUTION

Field Problem Description

The following field equations are given:

a) equilibrium [13],

$$\frac{\partial P}{\partial x} = -p_x(x) \quad , \tag{1}$$

where the axial resultant P is defined by

$$P \equiv \int_A \sigma dA \quad , \qquad \text{and} \quad (2)$$

$$p_x \equiv \oint_{S_c} T_x ds \quad ; \qquad (3)$$

b) strain-displacement relation

$$\varepsilon = \frac{\partial u}{\partial x} \quad ; \qquad (4)$$

c) thermomechanical constitution,

$$\sigma = E[\varepsilon - \alpha_1 - \alpha(T - T_R)] \quad , \qquad (5)$$

$$\frac{\partial \alpha_i}{\partial t} = \Omega_i(\varepsilon, T, \alpha_j) \quad , \quad i = 1,z \quad , \qquad \text{and} \quad (6)$$

$$q = -k \frac{\partial T}{\partial x} \quad ; \qquad (7)$$

where z is the total number of internal state variables; and

d) conservation of energy

$$\left[(E\varepsilon - E\alpha_1 + E\alpha T_R) \frac{\partial \alpha_1}{\partial t} + E\alpha^2 T \frac{\partial T}{\partial t}\right] - E\alpha T \frac{\partial \varepsilon}{\partial t} - \rho C_v \frac{\partial T}{\partial t} - \frac{\partial q}{\partial x} + \rho r = 0 \quad . \qquad (8)$$

The conservation of mass is satisfied trivially and the second law of thermodynamics has been previously shown to be satisfied by the above equations [14-16]. It should be noted that equilibrium equation (1) satisfies equilibrium in the axial coordinate direction only in an average sense over the cross-section.

The above 6+Z equations (excluding definition (3)) define a nonlinear initial-boundary value problem (together with appropriate thermal and mechanical initial and boundary conditions) in which the following dependent variables are sought as functions of x and t: σ, ε, u, q, T, P, and α_i.

For convenience the domain is defined to be of length L, so that boundary and initial conditions are of the form:

$$\left.\begin{aligned} u(x,0) &\equiv u_0^x = \text{known} \\ T(x,0) &\equiv T_0^x = \text{known} \end{aligned}\right\} \quad \text{initial conditions} \quad ; \tag{9}$$

and

$$\text{essential boundary conditions} \left\{\begin{aligned} &u(0,t) \equiv u_t^0 = \text{known or } P(0,t) \equiv P_t^0 = \text{known} \\ &u(L,t) \equiv u_t^L = \text{known or } P(L,t) \equiv P_t^L = \text{known} \\ &T(0,t) \equiv T_t^0 = \text{known or } q(0,t) \equiv q_t^0 = \text{known} \\ &T(L,t) \equiv T_t^L = \text{known or } q(L,t) \equiv q_t^L = \text{known} \end{aligned}\right\} \quad \text{natural boundary conditions.} \tag{10}$$

It is now assumed that $\sigma = \sigma(x)$ so that equation (2) reduces to

$$P = \sigma A \quad . \tag{11}$$

Therefore, substituting (4) into (5) and this result into (11) gives

$$P = EA\left[\frac{\partial u}{\partial x} - \alpha_1 - \alpha(T - T_R)\right] \quad . \tag{12}$$

The above result is now substituted into (1) to obtain

$$\frac{\partial}{\partial x}\left\{EA\left[\frac{\partial u}{\partial x} - \alpha_1 - \alpha(T - T_R)\right]\right\} = -p_x(x) \quad , \tag{13}$$

which represents the differential equation relating displacements and temperature to the applied load $p_x(x)$.

Equations (4) and (7) are next substituted into energy balance law (8) and this result is integrated over the cross-sectional area A to obtain

$$A\left[\left(E\frac{\partial u}{\partial x} - E\alpha_1 + E\alpha T_R\right)\frac{\partial \alpha_1}{\partial t} + E\alpha^2 T\frac{\partial T}{\partial t}\right] - AE\alpha T\frac{\partial^2 u}{\partial t \partial x} - A\rho C_v\frac{\partial T}{\partial t}$$

$$+ A\frac{\partial}{\partial x}\left(k\frac{\partial T}{\partial x}\right) = -A\rho r \quad , \tag{14}$$

where it has been assumed that all field variables depend on x and t only.

Now define

$$Q \equiv \int_A q\, dA = -\int_A k\frac{\partial T}{\partial x}\, dA = -k\frac{\partial T}{\partial x}A \quad . \tag{15}$$

Careful inspection of equations (13) and (14) will indicate that these equations, together with internal state variable growth laws (6) and initial and boundary conditions (9) and (10), represent a well-posed boundary value problem in terms of the 2+z dependent variables u, T, and α_i.

Solution Procedure

The field problem is to be solved analytically using the semi-discretized finite element technique with timewise finite differencing. In order to accomplish this, differential equations (13) and (14) must first be written in a suitable variational form.

Variational Equations

Consider first equation (13). This governing equation is integrated against a suitably smooth test function $v = v(x)$ over the domain of some element Ω_e: $x_e < x < x_{e+1}$:

$$\int_{x_e}^{x_{e+1}} v \left[\frac{\partial}{\partial x} \left\{ EA \left[\frac{\partial u}{\partial x} - \alpha_1 - \alpha(T - T_R) \right] \right\} + p_x \right] dx = 0 \quad . \tag{16}$$

Integrating by parts results in

$$- \int_{x_e}^{x_{e+1}} EA \frac{\partial v}{\partial x} \left[\frac{\partial u}{\partial x} - \alpha_1 - \alpha(T - T_R) \right] dx = - \left| v \, EA \left[\frac{\partial u}{\partial x} - \alpha_1 - \alpha(T - T_R) \right] \right|_{x_e}^{x_{e+1}}$$

$$- \int_{x_e}^{x_{e+1}} v \, p_x dx \quad . \tag{17}$$

Substituting equation (12) into the boundary term thus results in

$$- \int_{x_e}^{x_{e+1}} EA \frac{\partial v}{\partial x} \left[\frac{\partial u}{\partial x} - \alpha_1 - \alpha(T - T_R) \right] dx =$$

$$-v(x_{e+1}) \, P(x_{e+1}) + v(x_e) \, P(x_e) - \int_{x_e}^{x_{e+1}} v \, p_x dx \quad . \tag{18}$$

Now consider equation (14). Once again the governing equation is integrated against a suitably smooth test function $w = w(x)$ over the domain of the element Ω_e:

$$\int_{x_e}^{x_{e+1}} w \left\{ A \left[\left(E \frac{\partial u}{\partial x} - E\alpha_1 + E\alpha T_R \right) \frac{\partial \alpha_1}{\partial t} + E\alpha^2 \, T \frac{\partial T}{\partial t} \right] \right.$$

$$\left. -AE\alpha T \frac{\partial^2 u}{\partial t \partial x} - A\rho C_v \frac{\partial T}{\partial t} + A \frac{\partial}{\partial x} \left(k \frac{\partial T}{\partial t} \right) + A \, \rho r \right\} dx = 0 \quad . \tag{19}$$

Integrating the heat flux term by parts results in

$$\int_{x_e}^{x_{e+1}} \left\{ -kA \frac{\partial w}{\partial x} \frac{\partial T}{\partial x} + wA \left[\left(E \frac{\partial u}{\partial x} - E\alpha_1 + E\alpha T_R \right) \frac{\partial \alpha_1}{\partial t} + E\alpha^2 T \frac{\partial T}{\partial t} \right. \right.$$

$$\left. \left. -E\alpha T \frac{\partial^2 u}{\partial t \partial x} \right] \right\} dx = w(x_{e+1})\, Q(x_{e+1}) - w(x_e)\, Q(x_e)$$

$$+ \int_{x_e}^{x_{e+1}} wA \left(\rho C_v \frac{\partial T}{\partial t} - \rho r \right) dx \quad , \tag{20}$$

where equation (15) has been substituted into the boundary terms.

Finite Element Spacial Discretization

Quadratic displacement and linear temperature fields are now chosen within each element:

$$u(x,t) = \sum_{i=1}^{3} u_i^e \psi_i^e \quad , \quad x_e < x < x_{e+1} \quad , \text{ and} \tag{21}$$

$$T(x,t) = \sum_{i=1}^{2} T_i^e \phi_i^e \quad , \quad x_e < x < x_{e+1} \quad , \tag{22}$$

where $u_i^e = u_i^e(t)$ and $T_i^e = T_i^e(t)$ are the nodal displacements and temperatures, respectively, and $\psi_i^e = \psi_i^e(x)$ and $\phi_i^e = \phi_i^e(x)$ are quadratic and linear shape functions, respectively [17].

Appropriately, v and w are endowed with the properties of u and T, respectively, so that

$$v \equiv \psi_i^e \quad i = 1,2,3$$

$$w \equiv \phi_i^e \quad i = 1,2 \qquad . \tag{23}$$

Substitution of equations (12) and (21) through (23) into variational principle (18) results in

$$-\int_{x_e}^{x_{e+1}} EA \frac{d\psi_i^e}{dx} \left[\frac{\partial}{\partial x} \left(\sum_{j=1}^{3} u_j^e \psi_j^e \right) - \alpha_1 \right.$$

$$\left. -\alpha \left(\sum_{j=1}^{2} T_j^e \phi_j^e - T_R \right) \right] dx = - \psi_i^e(x_{e+1}) P(x_{e+1}) + \psi_i^e(x_e) P(x_e)$$

$$- \int_{x_e}^{x_{e+1}} \psi_i^e p_x dx \quad , \quad i = 1,2,3 \quad . \tag{24}$$

The above may be written in the following compact form

$$\sum_{j=1}^{3} K_{ij}^e u_j^e + \sum_{j=1}^{2} S_{ij}^e T_j^e = F_i^e \quad , \quad i = 1,2,3, \tag{25}$$

where

$$K_{ij}^e \equiv - \int_{x_e}^{x_{e+1}} EA \frac{d\psi_i^e}{dx} \frac{d\psi_j^e}{dx} dx \qquad i = 1,2,3; \; j = 1,2,3 \quad ; \tag{26}$$

$$S_{ij}^e \equiv \int_{x_e}^{x_{e+1}} EA\alpha \frac{d\psi_i^e}{dx} \phi_j^e dx \qquad i = 1,2,3; \; j = 1,2 \quad ; \tag{27}$$

$$F_i^e \equiv \int_{x_e}^{x_{e+1}} EA \frac{d\psi_i^e}{dx} (-\alpha_1 + \alpha T_R) dx$$

$$-P(x_i) - \int_{x_e}^{x_{e+1}} \psi_i^e \, p_x dx \quad , \qquad i = 1,2,3. \tag{28}$$

Similarly, substitution of equations (21) through (23) into equation (20) results in

$$\int_{x_e}^{x_{e+1}} \left\{ -kA \frac{d\phi_i^e}{dx} \frac{\partial}{\partial x} \left(\sum_{j=1}^{2} T_j^e \phi_j^e \right) + A \, \phi_i^e \left[\left(E \frac{\partial}{\partial x} \left(\sum_{j=1}^{3} u_j^e \psi_j^e \right) - E\alpha_1 \right.\right.\right.$$

$$\left. + E\alpha T_R \right) \frac{\partial \alpha_1}{\partial t} + E\alpha^2 \left(\sum_{j=1}^{2} T_j^e \phi_j^e \right) \frac{\partial}{\partial t} \left(\sum_{m=1}^{2} T_m^e \phi_m^e \right)$$

$$\left.\left.\left. - E\alpha \left(\sum_{j=1}^{2} T_j^e \phi_j^e \right) \frac{\partial^2}{\partial t \partial x} \left(\sum_{m=1}^{3} u_m^e \psi_m^e \right) \right] \right\} dx =$$

$$\phi_i^e(x_{e+1}) \, Q(x_{e+1}) - \phi_i^e(x_e) \, Q(x_e) + \int_{x_e}^{x_{e+1}} \phi_i^e \, A \left[\rho C_v \frac{\partial}{\partial t} \left(\sum_{m}^{2} T_m^e \phi_m^e \right) - \rho r \right] dx,$$

$$i = 1,2. \tag{29}$$

Equations (29) may be written in the following form:

$$\sum_{j=1}^{3} \overline{K}_{ij}^e \, u_j^e + \sum_{j=1}^{2} \overline{S}_{ij}^e \, T_j^e + \int_{x_e}^{x_{e+1}} \phi_i^e \, A \left[E\alpha^2 \left(\sum_{j=1}^{2} T_j^e \, \phi_j^e \right) \left(\sum_{m=1}^{2} \frac{dT_m^e}{dt} \phi_m^e \right) \right.$$

$$-E\alpha\left(\sum_{j=1}^{2} T_j^e \phi_j^e\right)\left(\sum_{m=1}^{3} \frac{du_m^e}{dt}\frac{d\psi_m^e}{dx}\right) - \rho C_v\left(\sum_{m=1}^{2} \frac{dT_m^e}{dt}\phi_m^e\right) + \rho r\Bigg] dx$$

$$= -\int_{x_e}^{x_{e+1}} \phi_i^e A(-E\alpha_1 + E\alpha T_R)\frac{\partial \alpha_1}{\partial t} - Q(x_i) \quad , \qquad i = 1,2, \tag{30}$$

where

$$\overline{K}_{ij}^e \equiv \int_{x_e}^{x_{e+1}} AE\ \phi_i^e \frac{d\psi_j^e}{dx}\frac{\partial \alpha_1}{\partial t}\, dx \qquad i = 1,2;\ j = 1,2,3; \text{ and} \tag{31}$$

$$\overline{S}_{ij}^e \equiv -\int_{x_e}^{x_{e+1}} kA \frac{d\phi_i^e}{dx}\frac{d\phi_j^e}{dx}\, dx \quad ; \quad i = 1,2;\ j = 1,2. \tag{32}$$

Finite Difference Timewise Discretization

Time dependence in equations (6) and (30) is handled via finite differencing. Although higher order approximations may be used, Euler forward difference approximations are now entered for the time rate of change of α_k^e, T_m^e, and u_m^e.

$$\frac{\partial \alpha_k^e}{\partial t}(x,t) \cong [\alpha_k^e(x,t+\Delta t) - \alpha_k^e(x,t)]/\Delta t, \qquad k = 1, \ldots, z \tag{33}$$

$$\frac{dT_m^e}{dt}(t) \cong [T_m^e(t+\Delta t) - T_m^e(t)]/\Delta t, \qquad m = 1,2\ , \qquad \text{and} \tag{34}$$

$$\frac{du_m^e}{dt}(t) \cong [u_m^e(t+\Delta t) - u_m^e(t)]/\Delta t, \qquad m = 1,2,3. \tag{35}$$

Substitution of (33) through (35) into finite element equations (30) gives

$$\sum_{j=1}^{3} \bar{K}_{ij}^{e} u_j^e + \sum_{j=1}^{2} \bar{S}_{ij}^{e} T_j^e$$

$$+ \int_{x_e}^{x_{e+1}} A\phi_i^e \left\{ E\alpha^2 \left[\sum_{j=1}^{2} T_j^e \phi_j^e \right] \left[\sum_{m=1}^{2} \left(\frac{T_m^e(t+\Delta t) - T_m^e(t)}{\Delta t} \right) \phi_m^e \right] \right.$$

$$- E\alpha \left[\sum_{j=1}^{2} T_j^e \phi_j^e \right] \left[\sum_{m=1}^{3} \left(\frac{u_m^e(t+\Delta t) - u_m^e(t)}{\Delta t} \right) \frac{\partial \psi_m^e}{\partial x} \right]$$

$$\left. - \rho C_v \left[\sum_{m=1}^{2} \left(\frac{T_m^e(t+\Delta t) - T_m^e(t)}{\Delta t} \right) \phi_m^e \right] + \rho r \right\} dx$$

$$= - \int_{x_e}^{x_{e+1}} A\phi_i^e \left[-E\alpha_1(t) + E\alpha T_R \right] \frac{\partial \alpha_1}{\partial t}(t)$$

$$- Q(x_i) \quad , \qquad i = 1,2 \, . \tag{36}$$

The above may be written as follows:

$$\sum_{j=1}^{3} \bar{K}_{ij}^{e} u_j^e + \sum_{j=1}^{2} \bar{S}_{ij}^{e} T_j^e$$

$$+ \sum_{k=1}^{2} \sum_{j=1}^{2} C_{ijk} T_j^e T_k^e + \sum_{j=1}^{2} D_{ij} T_j^e$$

$$+ \sum_{k=1}^{2} \sum_{j=1}^{3} E_{ikj} T_k^e u_j^e + \sum_{j=1}^{2} G_{ij} T_j^e$$

$$+ \sum_{j=1}^{2} H_{ij} T_j^e = \bar{F}_i^e \quad , \qquad i = 1,2, \tag{37}$$

where

$$C_{ijk} \equiv \int_{x_e}^{x_{e+1}} A\phi_i^e \frac{E\alpha^2}{\Delta t} \phi_j^e \phi_k^e \, dx \quad , \qquad i = 1,2;\ j = 1,2;\ k = 1,2 \ , \quad (38)$$

$$D_{i1} \equiv - \int_{x_e}^{x_{e+1}} A\phi_i^e \frac{E\alpha^2}{\Delta t} [T_1^e(t)(\phi_1^e)^2 + T_2^e(t)\ \phi_1^e\phi_2^e] \, dx, \qquad i = 1,2 \ , \quad (39)$$

$$D_{i2} \equiv - \int_{x_e}^{x_{e+1}} A\phi_i^e \frac{E\alpha^2}{\Delta t} [T_1^e(t)\phi_1^e\phi_2^e + T_2^e(t)(\phi_2^e)^2] \, dx, \qquad i = 1,2 \ , \quad (40)$$

$$E_{ikj} \equiv - \int_{x_e}^{x_{e+1}} A\phi_i^e \frac{E\alpha}{\Delta t} \phi_k^e \frac{\partial \psi_j^e}{\partial x} \, dx \quad , \qquad i = 1,2,;\ k = 1,2;\ j = 1,2,3 , \quad (41)$$

$$G_{i1} \equiv \int_{x_e}^{x_{e+1}} A\phi_i^e \frac{E\alpha}{\Delta t} \left[u_1^e(t)\ \phi_1^e \frac{\partial \psi_1^e}{\partial x} + u_2^e(t)\ \phi_1^e \frac{\partial \psi_2^e}{\partial x} + u_3^e(t)\ \phi_1^e \frac{\partial \psi_3^e}{\partial x} \right] dx, \ i = 1,2 \ , \quad (42)$$

$$G_{i2} \equiv \int_{x_e}^{x_{e+1}} A\phi_i^e \frac{E\alpha}{\Delta t} \left[u_1^e(t)\phi_2^e \frac{\partial \psi_1^e}{\partial x} + u_2^e(t)\phi_2^e \frac{\partial \psi_2^e}{\partial x} + u_3^e(t)\phi_2^e \frac{\partial \psi_3^e}{\partial x} \right] dx \ , \ i = 1,2 \ , \quad (43)$$

$$H_{ij} \equiv - \int_{x_e}^{x_{e+1}} A\phi_i^e \frac{\rho C_v}{\Delta t} \phi_j^e \, dx \quad , \qquad i = 1,2;\ j = 1,2; \qquad \text{and} \quad (44)$$

$$\overline{F}_i^e \equiv - \int_{x_e}^{x_{e+1}} A\phi_i^e \left[\frac{\rho C_v}{\Delta t} \left(\sum_{j=1}^{2} T_j^e(t)\phi_j^e \right) + \rho r \right] dx$$

$$- \int_{x_e}^{x_{e+1}} A\phi_i^e \left[-E\alpha_1(t) + E\alpha T_R \right] \frac{\partial \alpha_1}{\partial t}(t) \, dx$$

$$- Q(x_i) \qquad i = 1,2 \ . \quad (45)$$

Equations (37) may be written equivalently as follows:

$$\sum_{j=1}^{3} \overline{\overline{K}}^{e}_{ij} \, u^{e}_{j} + \sum_{j=1}^{2} \overline{\overline{S}}^{e}_{ij} \, T^{e}_{j} = \overline{F}^{e}_{i} \quad , \tag{46}$$

where K^{e}_{ij} and $\overline{F}^{e}_{i}$ are as defined previously, and

$$\overline{\overline{K}}^{e}_{ij} \equiv \overline{K}^{e}_{ij} + \sum_{k=1}^{2} E_{ikj} \, T^{e}_{k} \quad , \quad \text{and} \tag{47}$$

$$\overline{\overline{S}}^{e}_{ij} \equiv \overline{S}^{e}_{ij} + \sum_{k=1}^{2} C_{ijk} \, T^{e}_{k} + D_{ij} + G_{ij} + H_{ij} \quad . \tag{48}$$

The above equations may be adjoined with equations (25) to obtain the following set of nonlinear equations for each element.

$$\underbrace{\left[\begin{array}{c|c} K^{e} & S^{e} \\ \hline \overline{\overline{K}}^{e} & \overline{\overline{S}}^{e} \end{array}\right]}_{\substack{2\times 3 \quad 2\times 2 \\ 5\times 5}} \left\{\begin{array}{c} u^{e} \\ \hline T^{e} \end{array}\right\}_{5\times 1} = \left\{\begin{array}{c} F^{e} \\ \hline \overline{F}^{e} \end{array}\right\}_{5\times 1} \tag{49}$$

where all nonlinearity is contained in $[\overline{\overline{S}}]$, $\{F^{e}\}$, and $\{\overline{F}^{e}\}$.

Global Assembly and Boundary Conditions

Global assembly is accomplished in the standard way using the Boolean matrix [17]. Interelement continuity is guaranteed by setting

$$P^{e}_{2} + P^{e+1}_{1} = 0 \quad , \quad \text{and} \tag{50}$$

$$\phi^{e}_{2} + \phi^{e+1}_{1} = 0 \quad . \tag{51}$$

Boundary conditions are implemented in the standard way: 1) essential boundary conditions are handled by placing one on the diagonal of the

appropriate row and zeros off diagonal in the stiffness matrix, and the specified value of the essential variable on the right hand side; and 2) natural boundary conditions are implemented directly to the right hand side.

Solution of the Nonlinear Algebraic System

Initial conditions are used for the first time step. The time step Δt is supplied for each load increment and boundary conditions are incremented directly from supplied input functions.

The internal state variable α_1 is handled in equations (23) and (45) by using equations (35). α_1 is initialized according to reference 18. The nonlinear stiffness matrix $[\bar{\bar{S}}]$ is initialized using nodal temperatures and displacements from the previous time step. The displacements and temperatures at time $t+\Delta t$ are then estimated directly and without iteration by utilizing equations (49) for very small time steps.

EXAMPLE PROBLEMS

In order to completely define an example problem it is necessary to specify internal state variable growth laws (6). Numerous models have been proposed for crystalline metals [18,19]. Since it is not the purpose of this research to compare these models, a relatively established model proposed by Bodner and Partom [20] has been chosen. This model contains two internal state variables: the inelastic strain (α_1) and the drag stress (α_2). The growth laws for these variables are given by

$$\dot{\alpha}_1 = \frac{2}{3} D_o \frac{\sigma}{|\sigma|} \exp\left[-\left(\frac{n+1}{2n}\right)\left(\frac{\alpha_2}{\sigma}\right)^{2n}\right] \tag{52}$$

and

$$\dot{\alpha}_2 = m(Z_1 - \alpha_2)\,\sigma\dot{\alpha}_1 - AZ_1\left(\frac{\alpha_2 - Z_1}{Z_I}\right)^r , \tag{53}$$

where D_0, n, m, Z_I, Z_I, and r are experimentally determined material constants.

For the purpose of modeling the temperature gradient in a specific component, a hypothetical problem has been chosen using material properties representative of Inconel 100 at 1005°k (1350°F). The material and geometric properties are given in Table I. The geometry is representative of a cylindrical uniaxial bar which is 2.50 inches long and 0.25 inches in diameter. It has previously been shown that Bodner and Partom's model accurately predicts the stress-strain behavior of IN100 under uniaxial loading conditions for both monotonic and cyclic strain controlled loadings [12,18].

ρC_v = 5.032 MPa/°K

α = 13.14×10^{-6} in/in/°K

$k = 21.0 \times 10^{-6} \frac{\text{MPa M}^2}{\text{sec°K}}$

E = 146.86×10^{3} MPa

A = 7.12557×10^{-5} m^2

T_R = 1005°K

L = .06350 m

D_0 = 10×10^{3} in/in

n = 0.70

m = 2.57

Z_1 = 1015.0

Z_I = 600.0

r = 2.66

Table I. Material Properties for IN 100 at 1005°K (1350°F)

Utilizing the material properties described above, the following effects have been studied using the model developed herein:

1) the effect of variation of strain rate on the time dependence of temperature at the midpoint of a monotonically extended uniaxial bar which is insulated on the longitudinal boundaries [Figs. 1-4];

2) the spacial variation of temperature for the case above [Fig. 5];

and

3) the effect of end temperature boundary conditions on the temperature at the center of a uniaxial bar which is held at fixed temperature at the end points and subjected to cyclically imposed end displacements [Figs. 8 and 9].

Examples 1 and 2 are constructed primarily to determine the effects of thermomechanical heating on the stress-strain behavior of uniaxial constitutive specimens. It is found in examples 1 and 2 that if a specimen is mounted in an experimental apparatus which has massive grips simulating a fixed temperature boundary condition there can be substantial axial temperature gradients induced in a time dependent boundary layer near the ends of the specimen. On the other hand, these boundary conditions do not appear to substantially affect the predicted stress-strain behavior, especially when the strain measurement is taken between the thermal boundary layers near the grips. Therefore, it would appear that the standard procedure for obtaining stresses and strains in uniaxial bars is not substantially affected by mechanically induced, axial temperature gradients when the grips are at fixed temperature equivalent to the initial specimen temperature and the bar is loaded monotonicalaly. However, it should be noted that massive grips which are mounted outside a furnace could, by their much lower temperature

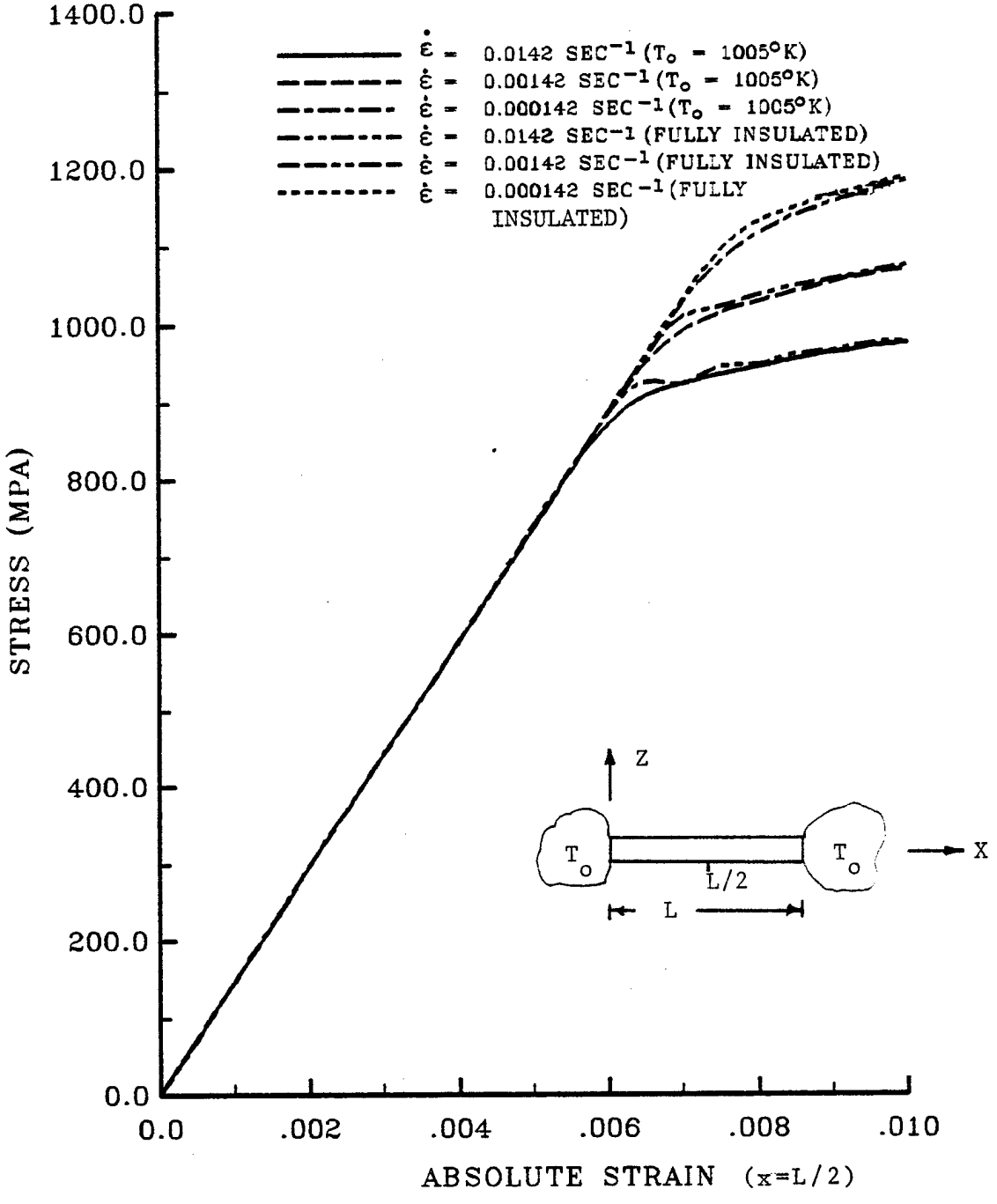

Fig. 1. Predicted Stress vs. Strain for a Uniaxial Bar Pulled at Various Constant Strain Rates.

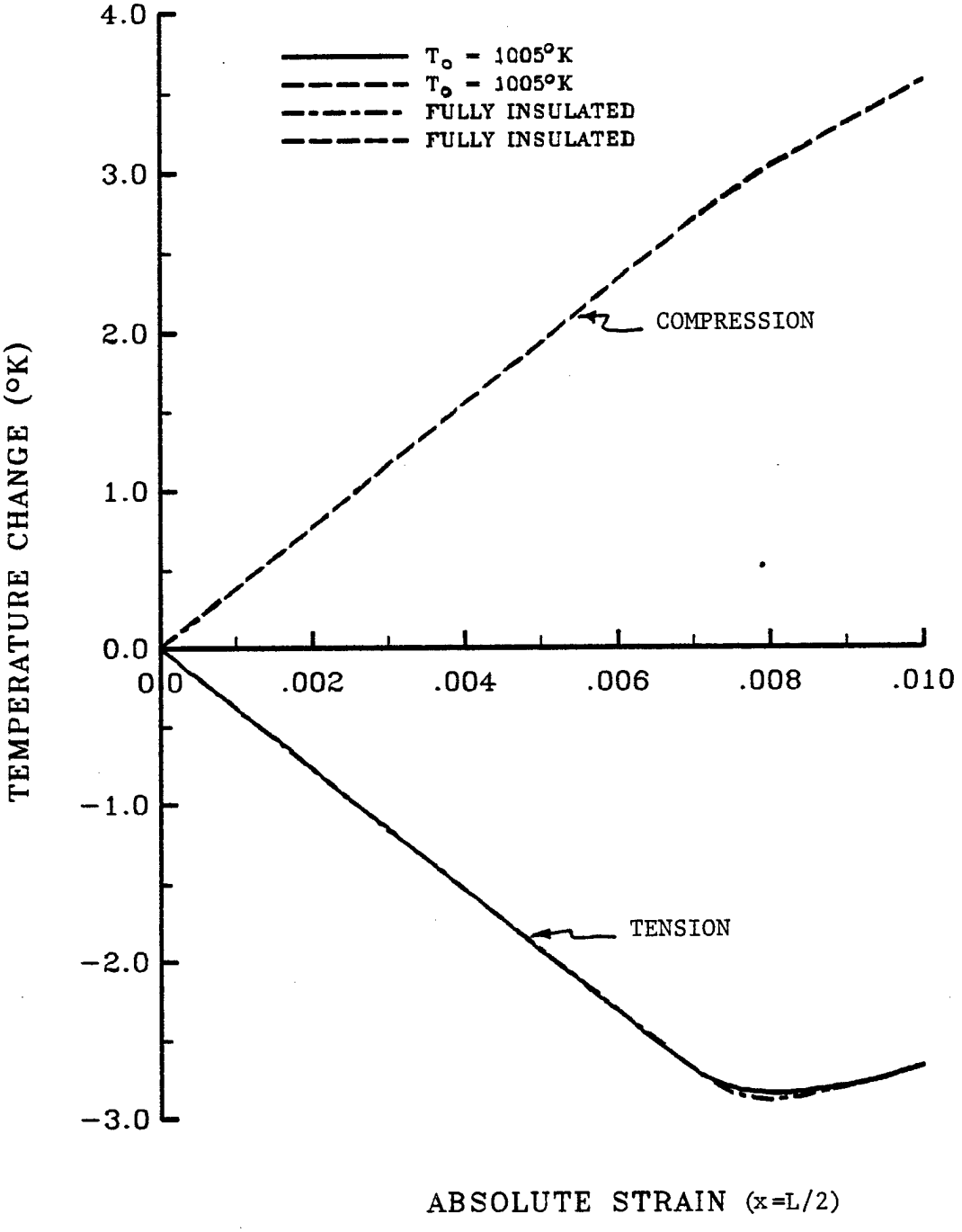

Fig. 2. Predicted Temperature vs. Absolute Strain for Monotonic Deformation Histories Described in Fig.1. ($\dot{\varepsilon} = \pm .0142$ sec^{-1})

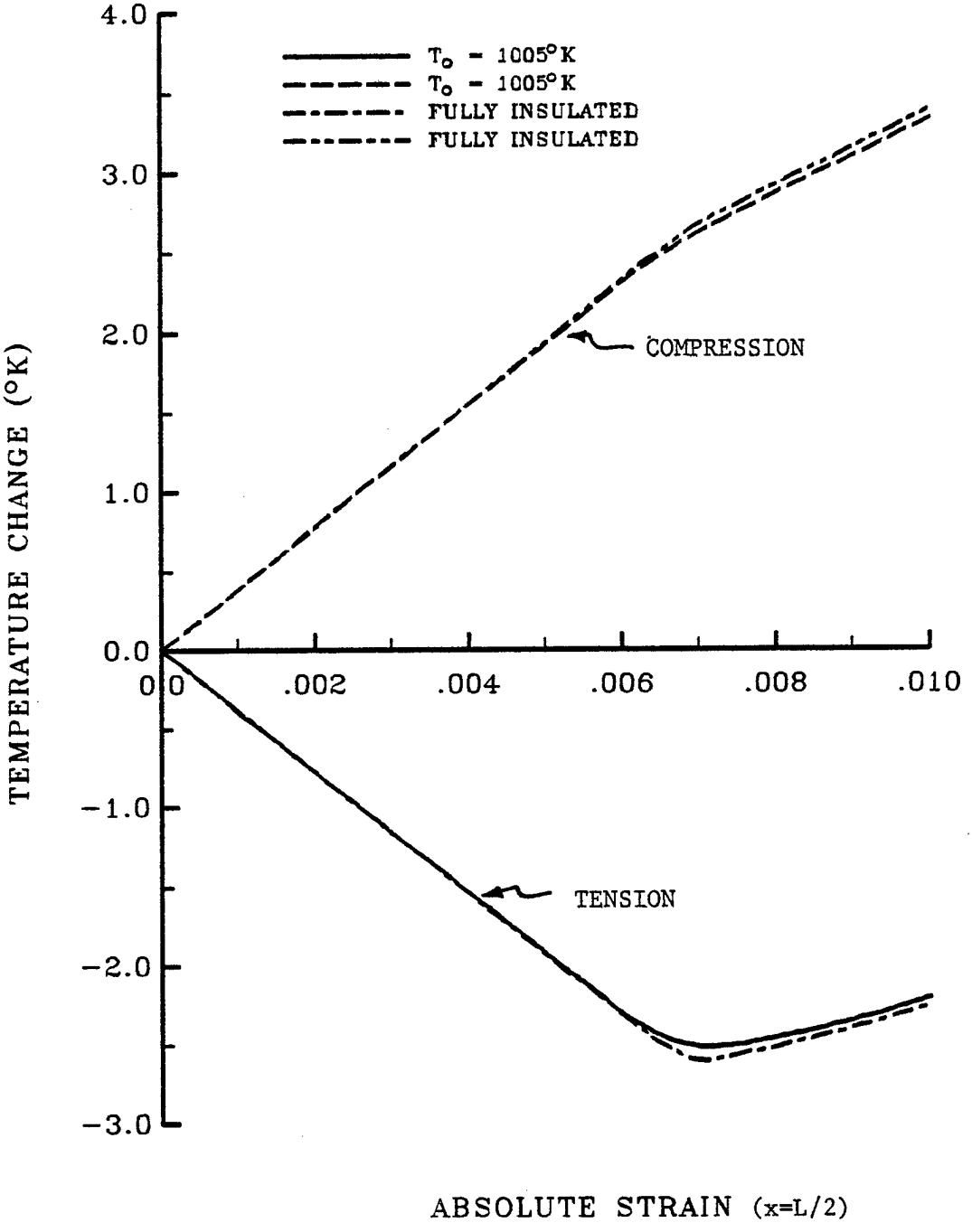

Fig. 3. Predicted Temperature vs. Absolute Strain for Monotonic Deformation Histories Described in Fig. 1. ($\dot{\varepsilon}$= $\pm$.00142 sec^{-1})

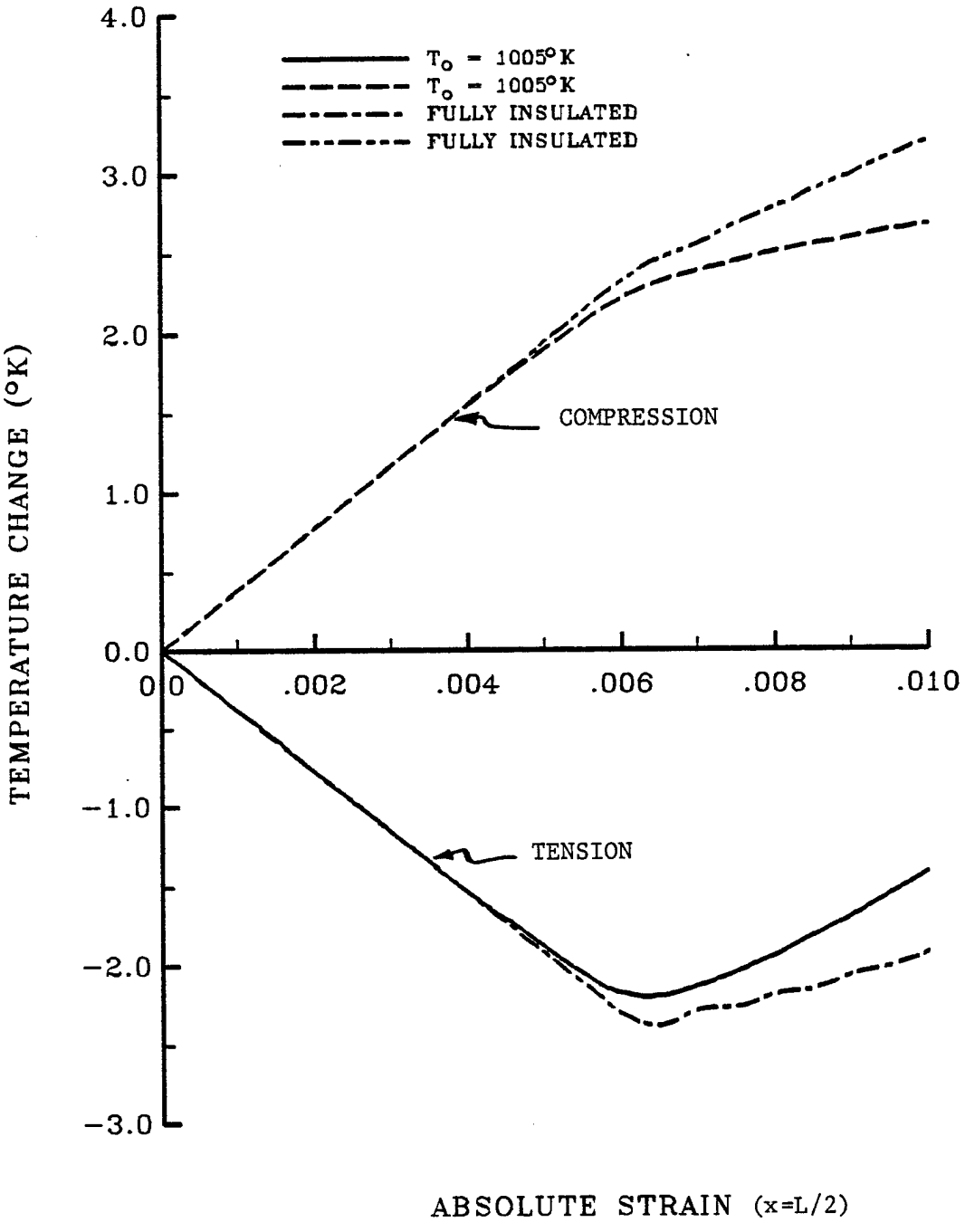

Fig. 4. Predicted Temperature vs. Absolute Strain for Monotonic Deformation Histories Described in Fig. 1. ($\dot{\varepsilon}$= $\pm$.000142 sec^{-1})

than the initial speciman temperature, may induce significant error in predicted strains if the strain is measured by dividing relative displacement by some gage length.

The final example demonstrates that under cyclic loading conditions the above conclusions may not necessarily be true, especially when the specimen is subjected to high-cycle fatigue and at high strain rates. There is definitely a trend towards an increasing mean temperature in the bar, and this mean temperature is strongly affected by the thermal boundary conditions as well as the loading rate. Although it would be interesting to determine the mean temperature rise in a cyclic fatigue test, the current algorithm precludes this analysis due to the extremely large computer times necessary to predict only a few cycles of response (approximately 43.8 CPU minutes on an Amdahl 470/V6 for the example demonstrated in Figs. 6 and 7).

Example 3 also demonstrates another interesting phenomenon which may be significant in large space structures. If the bar is perfectly insulated the mean temperature rise per cycle for the relatively slow loading rate shown in Fig. 6 is 3.7°K, whereas if the ends of the bar are held at a fixed temperature of 1005°K, the mean rise is 1.0°K per cycle. Faster loading rates show less difference between the adiabatic result and the fixed end temperature result. Since many of these structures are expected to be extremely flexible truss-like configurations, a typical metallic member which undergoes some yielding (which might be desirable in order to induce natural damping) might in fact undergo substantial enough heating during vibrational response such that the material properties could be adversely affected, thus resulting in a material related failure of the structure. However, further investigation is needed on this last issue since it is expected that the primary form of heat flux off of space structures will be via radiation on the longitudinal surfaces of the truss member. Since the current analysis

has treated these surfaces as insulated, no general statements can be made at this time regarding thermomechanical heating in space structures.

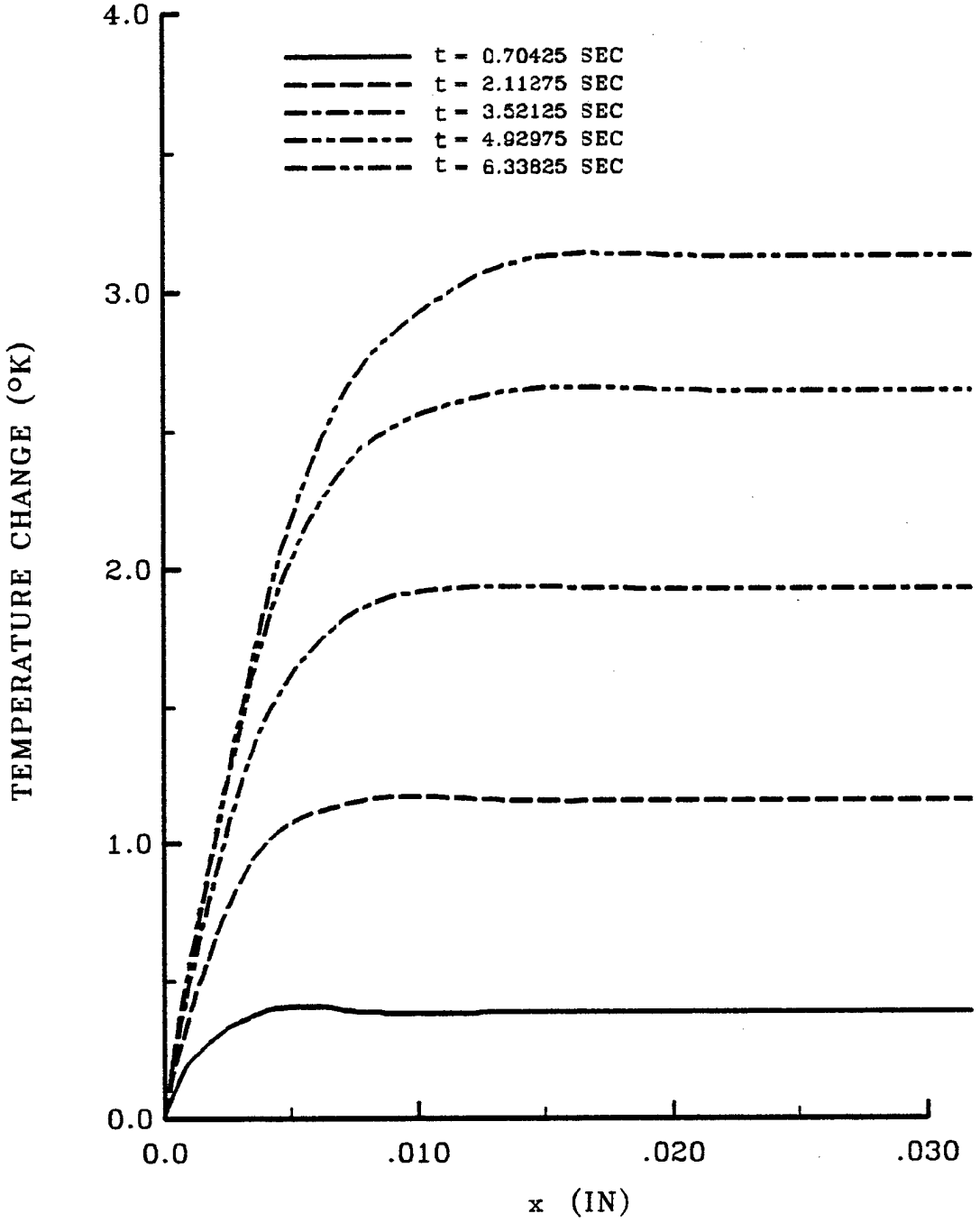

Fig. 5. Temperature vs. Spacial Location for Various Times for Constant Strain Rate $\dot{\varepsilon} = -.00142\ sec^{-1}$ (x = 0.3175 is the Midpoint of the Bar).

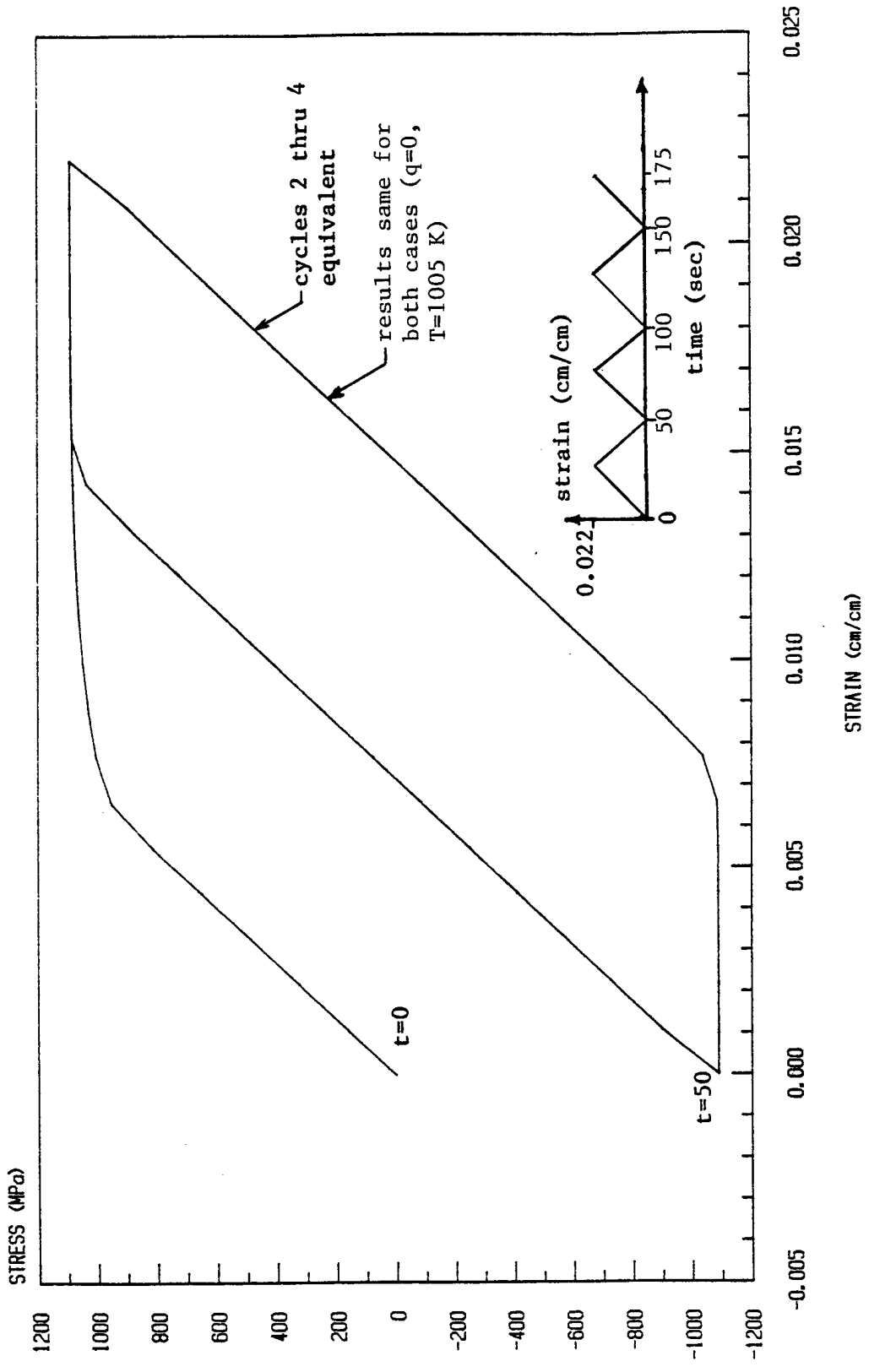

Fig. 6. Stress-Strain Curve and Strain input curve for cyclic load.

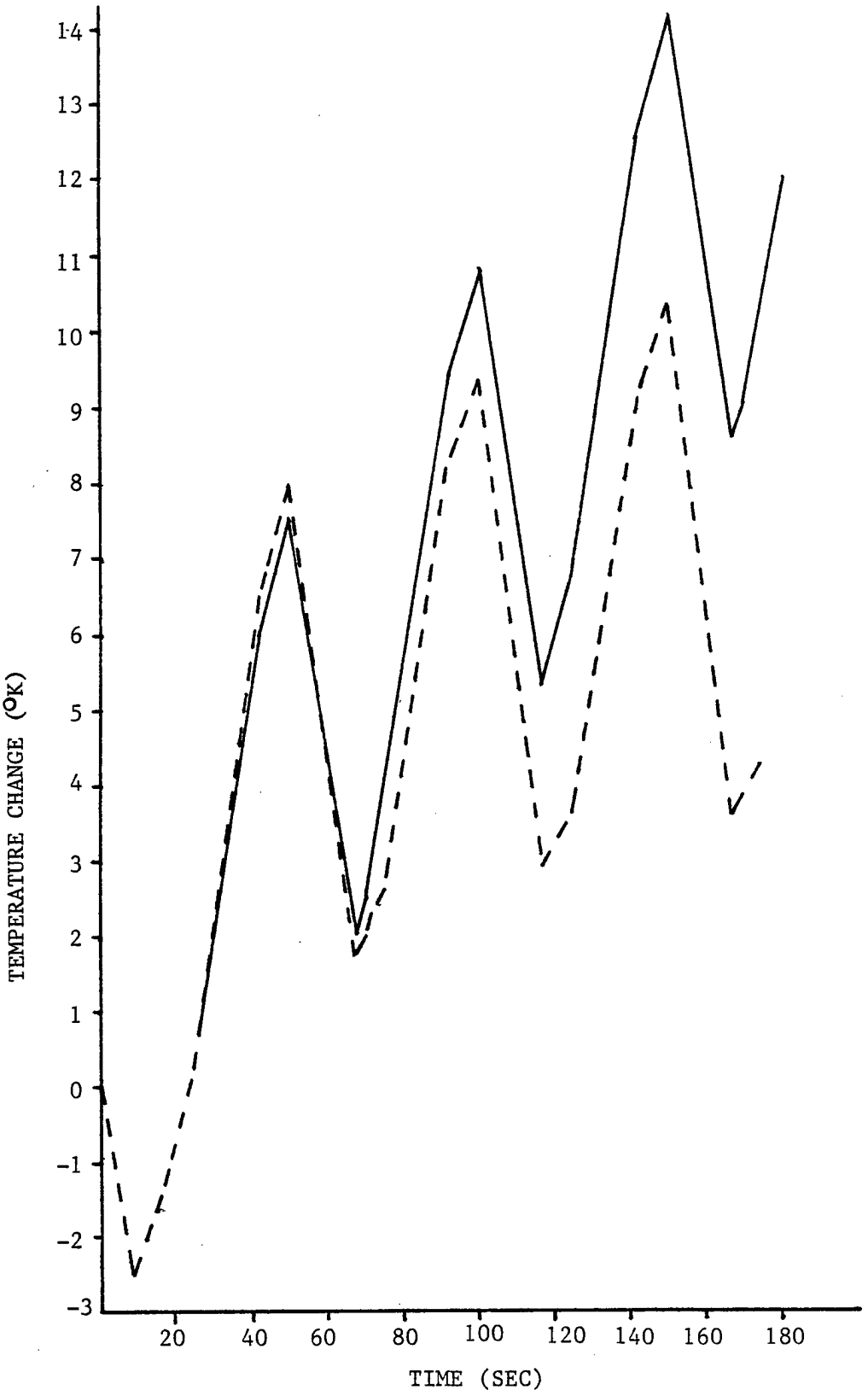

Fig. 7. Temperature Change at x=L/2 Versus Time for the Cyclically Loaded Bar Described in Fig. 6.

CONCLUSION

The current research has attemped to demonstrate the effects of mechanical loading on one-dimensional temperature gradients in a class of viscoplastic media. Due to the nonlinearity and stiffness of the field equations, it was necessary to utilize a numerical algorithm. This algorithm has been shown to be very inefficient for solving even one-dimensional examples. Therefore, it is apparent that significant refinement of the procedure will be necessary before multi-dimensional analyses can be performed by this method. Specifically, it would be significant to determine the effect of transverse temperature gradients on the stress-strain behavior of constitutive specimens. Furthermore, the effects of thermal boundary conditions on the longitudinal surface needs attention. The author is currently studying a perturbation technique for more efficient solution of these issues.

The above points notwithstanding, the current research demonstrates some important results. These are:

1) The axial temperature gradient in a viscoplastic uniaxial bar is strongly affected by the thermal boundary conditions on the ends.

2) The end temperature boundary conditions can cause temperature gradients which are substantial enough to induce spacial variations in stress and strains which invalidate the standard procedure of using average quantities, although when grips are mounted within a furnace at spacially constant temperature, it appears that the standard procedure is accurate.

3) There is a trend toward increasing average temperature in cyclically loaded bars; whether or not this effect is significant is strongly dependent on the thermal boundary conditions and the loading rate.

ACKNOWLEDGEMENT

The author gratefully acknowledges the support provided for this research by the Air Force Office of Scientific Research under contract no. F49620-83-C-0067.

REFERENCES

[1] J.M.C. Duhamel, Memoire sur le calcul des actions moleculaires developpees par les changements de temperature dan les corps solides. Memoires par divers savans, vol. 5, pp. 440-498, (1838).

[2] F. Neumann, Vorlesungen uber die theorie der elasticitat der festen Korper und des lichtathers. Leipzig, 107-120, (1885).

[3] B.A. Boley and J.H. Weiner, Theory of Thermal Stresses. Wiley, New York, (1960).

[4] O.W. Dillon, Jr., An experimental study of the heat generated during torsional oscillations. J. Mech. Phys. Solids, vol. 10, 235-244 (1962).

[5] O.W. Dillon, Jr., Temperature generated in aluminum rods undergoing torsional oscillations. J. Appl. Mech. 33, vol. 10, 3100-3105 (1962).

[6] O.W. Dillon, Jr., Coupled thermoplasticity. J. Mech. Phys. Solids, vol. 11, 21-33 (1963).

[7] G.R. Halford, Stored Energy of Cold Work Changes Induced by Cyclic Deformation. Ph.D. Thesis, University of Illinois, Urbana, Illinois (1966).

[8] O.W. Dillon, Jr., The heat generated during the torsional oscillations of copper tubes. Int. J. Solids Structures, vol. 2, 181-204 (1966).

[9] W. Olszak and P. Perzyna, Thermal Effects in Viscoplasticity. IUTAM Symp., East Kilbride, 206-212, Springer-Verlag, New York (1968).

[10] J. Kratochvil and R.J. DeAngelis, Torsion of a titanium elastic viscoplastic shaft. J. Appl. Mech. vol. 42, 1091-1097 (1971).

[11] E.P. Cernocky and E. Krempl, A theory of thermoviscoplasticity based on infinitesimal total strain. Int. J. Solids Structures, vol. 16, 723-741 (1980).

[12] D.H. Allen, A prediction of heat generation in a thermoviscoplastic uniaxial bar. Texas A&M University Mechanics and Materials Center Report no. MM 4875-83-10 (July 1983), (accepted for publication by Int. J. Solids Structures).

[13] D.H. Allen and W.E. Haisler, Introduction to Aerospace Structural Analysis. John Wiley (1985), in press.

[14] B.D. Coleman and M.E. Gurtin, Thermodynamics with internal state variables. J. Chem. Phys., vol. 47, 597-613 (1967).

[15] J. Kratochvil and O.W. Dillon, Jr., Thermodynamics of crystalline elastic-viscoplastic materials. J. Appl. Phys., vol. 41, 1470-1479 (1970).

[16] D.H. Allen, Thermodynamic constraints on the constitution of a class of thermoviscoplastic solids. Texas A&M University Mechanics and Materials Center, Report no. MM 12415-82-10, December (1982).

[17] J.N. Reddy, An Introduction to the Finite Element Method. McGraw-Hill, New York (1984).

[18] T.M. Milly and D.H. Allen, "A Comparative Study of Nonlinear Rate-Dependent Mechanical Constitutive Theories for Crystalline Solids at Elevated Temperatures, Virginia Polytechnic Institute and State University, March, 1982 (M.S. Thesis).

[19] D.H. Allen and J.M. Beek, "On the Use of Internal State Variables in Thermoviscoplastic Constitutive Equations," Proceedings 2nd Symposium on Nonlinear Constitutive Relations for High Temperature Applications, June, 1984.

[20] S.R. Bodner and Y. Partom, "Constitutive Equations for Elastic-Viscoplastic Strain-Hardening Materials," J. Appl. Mech, Vol. 42, 385-389 (1975).